Robotica (2015) volume 33, pp. 1351–1374. © Cambridge University Press 2014
doi:10.1017/S0263574714000769

Cross-coupled PID control in position domain for contour tracking

P. R. Ouyang*, T. Dam and V. Pano

Department of Aerospace Engineering, Ryerson University, Toronto, Canada

(Accepted February 24, 2014. First published online: April 1, 2014)

SUMMARY

Accurate contour tracking is one of the main tasks in modern manufacturing processes. By considering coupling effects among multiple axes, this paper proposes a cross-coupled proportional-integral-derivative (PID) control developed in position domain, and the controller is applied to a multi-axis computer numerical control (CNC) machine for contour tracking performance improvement. Stability analysis is conducted for the developed position domain cross-coupled PID control using the Lyapunov method, and guidelines for the selection of control gains are provided. The contour tracking performance are improved compared to an equivalent time domain controller, since the reference axis in position domain control does not contribute any error to the overall contouring error of the system. Simulation results demonstrate the effectiveness of cross-coupled PID position domain control for both linear and circular contour tracking, and prove the robustness of the controller to deal with random disturbances. It also shows that position domain cross-coupled PID control provides better contour tracking performance over position domain PID control and the equivalent time domain PID control.

KEYWORDS: Contour tracking; Position domain; PID control; Cross-coupled control; CNC machine.

1. Introduction

A common problem encountered by high-precision manufacturing processes is how to achieve good contour tracking performance of a machined product. Various control approaches have been developed to achieve good axial positioning accuracy.[1–8] Examples of control strategies that are commonly used in industry are, proportional-derivative (PD) control and proportional-integral-derivative (PID) control, feed-forward control, zero phase error tracking control, adaptive control, robust control, and others. These approaches typically involve controlling each axis of a multi-axis system independently. This may be preferred if the disturbance in one axis does not affect the performance of other axes in a multi-axis system. This, however, does not guarantee the reduction of the contour error for a multi-axis motion, as the lack of synchronization can lead to diminished contour accuracy of products as demonstrated in refs. [4–7].

Cross-coupled control (CCC) was introduced by Koren[4,5] to improve contour tracking performance. This method compensates the tracking errors for independent axis control by incorporating the contour error directly into the designed controller. Experiments have shown that CCC can achieve good contour tracking performances;[4–7] however, there are still tracking errors for each axis as shown in ref. [7]. Another control method called event-driven control[8–11] can produce synchronization among the motions of a multi-axis system, where certain events associated with one axial motion are used to trigger the control actions of all other axial motions in a synchronized manner. An event-driven controller uses an event or the arrival of a new measurement to trigger the controller to update the control action. The main advantage for event-driven control is the minimization of computer utilization and communication between system components. But it is particularly difficult to develop a system control theory for event-driven systems as mentioned in ref. [11].

* Corresponding author. E-mail: pouyang@ryerson.ca

https://doi.org/10.1017/S0263574714000769 Published online by Cambridge University Press

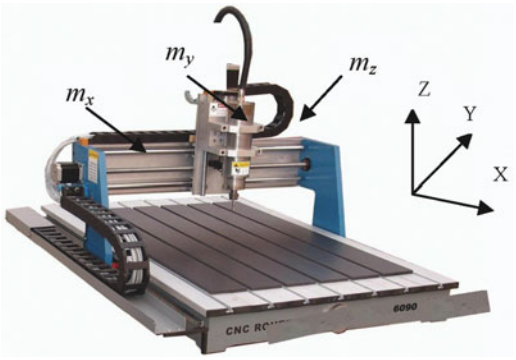


Fig. 1. Scheme of a CNC machine.

From the above discussion, it is concluded that these control methods have their advantages and disadvantages. In previous research, we proposed a PD position domain control (PDC) in ref. [13], and a PID PDC in ref. [14] for X-Y stage systems where only one slave motion was included in the system. Also, a PID with CCC for contour tracking control of a computer numerical control (CNC) system was introduced in ref. [15], but without proving the stability and without discussing the robustness of the control system. This research is an extension and complement of previous research, and the main motivation of this research is to take advantages of both CCC and PDC to form a new control system for multiple-DOF (degree of freedom) CNC machine systems. A new position domain cross-coupled PID control is proposed in this paper to improve contour tracking of a 3-axis CNC machine. One advantage of the cross-coupled PDC is to avoid the timing issue in a timed trajectory formulation that is overly restrictive for contour tracking tasks, and the other advantage of the proposed controller is to improve contour tracking performance by considering the coupling effects of the slave motions.

To formulate the PDC, the dynamic model of the multi-axis system is developed in position domain through a transformation from time domain to position domain. In this paper, the stability analysis is completed and simulation case studies are conducted for different contour profiles. One advantage of using PDC is that there is no tracking error for the reference axis, therefore the reference axis does not contribute error to the overall contouring error. Of course, to obtain an accurate contouring performance, a high-precision sensor is required to measure the displacement of the reference axis in order for a PDC system to be effectively utilized.

2. System Dynamic Model and Control Law

A general dynamic model of a 3-axis CNC system shown in Fig. 1 can be expressed as

$$\begin{cases} m_x\ddot{x} + c_x\dot{x} + k_x x + d_x = F_x(t) \\ m_y\ddot{y} + c_y\dot{y} + k_y y + d_y = F_y(t) \\ m_z\ddot{z} + c_z\dot{z} + k_z z + +d_z = F_z(t) \end{cases}, \tag{1}$$

where m_i, c_i, k_i, d_i, and F_i are the mass, damping coefficient, stiffness, disturbance, and driving force of the ith axis, respectively.

2.1. Time domain control

Since the assumed dynamic model shown in Fig. 1 is decoupled for each axis, a conventional PID controller in time domain control (TDC) can be applied to manipulate the motion of each axis independently.

$$\begin{cases} F_x = K^t_{P_x} e_x(t) + K^t_{I_x} \int_0^t e_x(\tau)\,d\tau + K^t_{D_x} \dot{e}_x(t) \\ F_y = K^t_{P_y} e_y(t) + K^t_{I_y} \int_0^t e_y(\tau)\,d\tau + K^t_{D_y} \dot{e}_y(t) \\ F_z = K^t_{P_z} e_z(t) + K^t_{I_z} \int_0^t e_z(\tau)\,d\tau + K^t_{D_z} \dot{e}_z(t) \end{cases}, \tag{2}$$

https://doi.org/10.1017/S0263574714000769 Published online by Cambridge University Press

where K_{Pi}^t, K_{Ii}^t, and K_{Di}^t are the proportional, integral, and derivative gains of the ith axis, respectively, with superscript t representing time domain.

2.2. Position domain control

In TDC, the trajectory for each axis is time-dependent and can be expressed as

$$\begin{cases} x(t) = f_x(t) \\ y(t) = f_y(t) \\ z(t) = f_z(t) \end{cases}. \tag{3}$$

The objective of PDC is to replace the time-dependency of the system with the dependency on one of its axes known as the reference or master axis. It should be mentioned that the master motion is controlled by traditional PD/PID control in time domain. The motions of all other axes, called slave axes, can be represented as functions of the motion of the master axis. Assuming that the X-axis is the reference axis, Eq. (3) can be rewritten in position domain, based on the contour shape, as

$$y(x) = g_y(x) \quad \text{and} \quad z(x) = g_z(x). \tag{4}$$

Equation (4) is the representation of a contour path in three dimensions that avoids the timing issue, as y and z are expressed as a function of position x; in other words, the motions of Y-axis and Z-axis follow the motion of the X-axis to form the designed contour profile.

Remark 1. Equation (4) can be used as a path planning method where the motion of the X-axis is the reference and the motions of Y-axis and Z-axis are the dependent motions. For the purposes of path planning, a lookup table, where the motions of Y and Z axes are related to the motion of the X-axis in a table, is used for the transformation of the desired axis trajectories from time domain to position domain. More specifically, the desired trajectory of each axis is initially defined as a function of time. Afterwards, the resulting trajectories are linearly interpolated with respect to the master axis' real trajectory. In this way the desired slave axes position is found for the equivalent master axis real trajectory.

Remark 2. For a master motion with complicated motion profiles, we can view the master motion as several segments where each segment is monotonically increasing (positive speed) or decreasing (negative speed), and the developed PDC can be used for the slave motions control in several contour segments. For example, for a circular contour, the master motion is divided into two segments: one segment is for the positive speed motion and the other is for the negative speed motion.

Remark 3. In this paper, we choose the X-axis as the master motion that is just for explanation purpose. In case there is no motion in the X-axis for a defined contour or the motion in the Y-axis is simple, we can choose the Y-axis as the master motion according to the defined contour profiles.

To formulate a control law described in position domain, it is necessary to define the relative velocity and relative acceleration in position domain from Eq. (4) as

$$y'(x) = \frac{\mathrm{d}g_y(x)}{\mathrm{d}x} \quad \text{and} \quad z'(x) = \frac{\mathrm{d}g_z(x)}{\mathrm{d}x}, \tag{5}$$

and

$$y''(x) = \frac{\mathrm{d}^2 g_y(x)}{\mathrm{d}x^2} \quad \text{and} \quad z''(x) = \frac{\mathrm{d}^2 g_z(x)}{\mathrm{d}x^2}. \tag{6}$$

From the definition, one can see that the velocity and acceleration can be represented as functions of the relative velocity and relative acceleration as follows:

$$\dot{y} = \frac{\mathrm{d}y}{\mathrm{d}t} = y'\dot{x} \quad \text{and} \quad \dot{z} = \frac{\mathrm{d}z}{\mathrm{d}t} = z'\dot{x}, \tag{7}$$

https://doi.org/10.1017/S0263574714000769 Published online by Cambridge University Press

and

$$\ddot{y} = \dot{x}^2 y'' + \ddot{x} y' \quad \text{and} \quad \ddot{z} = \dot{x}^2 z'' + \ddot{x} z'. \tag{8}$$

Substituting Eqs. (7) and (8) into Eq. (1) of the Y-axis and the Z-axis, the dynamics of two slave motions can be expressed as

$$\begin{cases} m_y \dot{x}^2 y''(x) + (m_y \ddot{x} + c_y \dot{x}) y'(x) + k_y y(x) + d_y = F_y(x) \\ m_z \dot{x}^2 z''(x) + (m_z \ddot{x} + c_z \dot{x}) z'(x) + k_z z(x) + d_z = F_z(x) \end{cases}. \tag{9}$$

The dynamics in Eq. (9) for slave motions is represented in position domain. An important conclusion of this transformation is that the dynamic model of the system in position domain is nonlinear, while the dynamic model in time domain is linear for the translational CNC system as shown in Fig. 1.

Similar to the traditional PID control law in Eq. (2) in time domain, a position domain PID control can be applied to Eq. (9) for contour tracking control. The control inputs F_i of the ith axis in position domain are also dependent on the reference axis position defined as follows:

$$\begin{cases} F_y(x) = K^p_{Py} e_y(x) + K^p_{Iy} \int_0^x e_y(s)\, ds + K^p_{Dy} e'_y(x) \\ F_z(x) = K^p_{Pz} e_z(x) + K^p_{Iz} \int_0^x e_z(s)\, ds + K^p_{Dz} e'_z(x) \end{cases}, \tag{10}$$

where K^p_{Pi}, K^p_{Ii}, and K^p_{Di} are the PID control gains, with superscript p representing position domain. Also, the contour error and its relative derivative are defined as

$$\begin{cases} e_y(x) = y_d(x) - y(x) \\ e_z(x) = z_d(x) - z(x) \end{cases} \quad \text{and} \quad \begin{cases} e'_y(x) = y'_d(x) - y'(x) \\ e'_z(x) = z'_d(x) - z'(x) \end{cases}. \tag{11}$$

The PDC law of Eq. (10) is similar to the TDC law of Eq. (2) in format but with some fundamental differences. The first difference is the domain that each controller uses; and the second difference is the derivative gains that have different physical meaning due to the differences between the derivative of the errors, $\dot{e}_i(t)$ and $e'_i(x)$, in TDC and PDC, respectively.

Substituting Eq. (11) into Eq. (10) gives the control law in the position domain where the X-axis is the reference, and considering Eq. (5), we have

$$\begin{cases} F_y(x) = K^p_{Py}(y_d(x) - y(x)) + K^p_{Iy} \int_0^x (y_d(s) - y(s)) ds + \frac{K^p_{Dy}}{\dot{x}} \dot{e}_y(x) \\ F_z(x) = K^p_{Pz}(z_d(x) - z(x)) + K^p_{Iz} \int_0^x (z_d(s) - z(s)) ds + \frac{K^p_{Dz}}{\dot{x}} \dot{e}_z(x) \end{cases}. \tag{12}$$

From Eq. (12) one can see that the PDC control law is equivalent to a nonlinear TDC control[12] when the master motion velocity is not constant. The stability of the PDC control is very important and its analysis is demonstrated in ref. [13] for a 2-DOF translational mechanism. In this paper, we will demonstrate that the PDC control can be extended to multiple-DOF systems through stability analysis.

2.3. Cross-coupled position domain PID control

If the CCC is added to PDC for contour tracking performance improvement, a cross-coupled PID PDC can be formed for controlling the coupled slave axes, Y- and Z-axes, as follows:

$$\begin{cases} F_y(x) = K^p_{Py} e_y + K^p_{Iy} \int_0^x e_y ds + K^p_{Dy} e'_y - W_y(K^c_{Py} e_c + K^c_{Dy} e'_c) \\ F_z(x) = K^p_{Pz} e_z + K^p_{Iz} \int_0^x e_z ds + K^p_{Dz} e'_z + W_z(K^c_{Pz} e_c + K^c_{Dz} e'_c) \end{cases}, \tag{13}$$

where K^c_{Pi} and K^c_{Di} are the CCC gains, with superscript c representing CCC, and e_c and e'_c being the contour error and the derivative of contour error, respectively. W_y and W_z are the coupling constants that depend on the controlled contour shape.

The difference between the tracking error and contour error is illustrated in Fig. 2 for a linear contour tracking problem. In Fig. 2, e is called the tracking error, defined as the distance between

https://doi.org/10.1017/S0263574714000769 Published online by Cambridge University Press

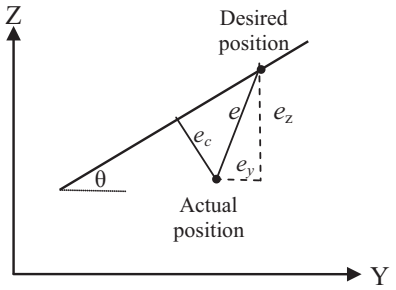


Fig. 2. Tracking and contour errors for a YZ-plane linear contour.

the desired position and the actual position; $e_y$and e_z are the tracking errors in the Y-axis and Z-axis, respectively. e_c is the contour error that is the shortest distance between the actual position and the desired contour.

In PDC/CCC, Y- and Z-axes are the slave axes and their errors are cross-coupled. Following the definition of a contour error in CCC derived in refs. [4–7], the contour errors for the slave motions (Y-axis and Z-axis) in position domain can be defined as follows:

$$e_c = -W_y e_y + W_z e_z \quad \text{and} \quad e'_c = -W_y e'_y + W_z e'_z, \tag{14}$$

where $W_y = \sin\theta$ and $W_z = \cos\theta$ for a linear motion. For a circular motion, $W_y = \sin\theta - \frac{e_y}{2R}$, $W_z = \cos\theta + \frac{e_z}{2R}$, and R is the radius of the tracked circular motion. θ is the angle in YZ plane between the Y-axis and the desired motion direction measured in a counter-clockwise direction. It should be mentioned that the angle θ is not constant for a nonlinear contour tracking motion, such as the circular motion.

3. Stability Analysis

3.1. Preparation

To facilitate the discussion, we have the following assumptions:

A1. The desired contour of $y_d(x)$ and $y_z(x)$ are of the third-order continuity for $x \in [x_{ini}, x_{fin}]$.
A2. The real tracking path in the X-axis $x(t)$ is of the third-order continuity for the contour.
A3. The disturbance $d_y(x)$ and $d_z(x)$are bounded in the full contour tracking process.

For the briefness of the stability analysis, the following notations are introduced and used in the following sections.

$$\|z\| = \max_{1\le i\le n} |z_i|, \quad \|A\| = \max_{1\le i\le n} |\lambda_i|,$$

$$M = \begin{bmatrix} m_y\dot{x}^2 & 0 \\ 0 & m_z\dot{x}^2 \end{bmatrix}, \quad C = \begin{bmatrix} m_y\ddot{x} + c_y\dot{x} & 0 \\ 0 & m_z\ddot{x} + c_z\dot{x} \end{bmatrix}, \quad K = \begin{bmatrix} k_y & 0 \\ 0 & k_z \end{bmatrix},$$

$$K_P^p = \begin{bmatrix} K_{Py}^p & 0 \\ 0 & K_{Pz}^p \end{bmatrix}, \quad K_I^p = \begin{bmatrix} K_{Iy}^p & 0 \\ 0 & K_{Iz}^p \end{bmatrix}, \quad K_D^p = \begin{bmatrix} K_{Dy}^p & 0 \\ 0 & K_{Dz}^p \end{bmatrix},$$

$$K_P^c = \begin{bmatrix} W_y^2 K_{Py}^c & -W_y W_z K_{Py}^c \\ -W_y W_z K_{Pz}^c & W_z^2 K_{Pz}^c \end{bmatrix}, \quad K_D^c = \begin{bmatrix} W_y^2 K_{Dy}^c & -W_y W_z K_{Dy}^c \\ -W_y W_z K_{Dz}^c & W_z^2 K_{Dz}^c \end{bmatrix},$$

$$\overline{C} = \left(C + K_D^p + K_D^c\right)$$

$$= \begin{bmatrix} m_y\ddot{x} + c_y\dot{x} + K_{Dy}^p + W_y^2 K_{Dy}^c & -W_y W_z K_{Dy}^c \\ -W_y W_z K_{Dz}^c & m_z\ddot{x} + c_z\dot{x} + K_{Dz}^p + W_z^2 K_{Dz}^c \end{bmatrix},$$

https://doi.org/10.1017/S0263574714000769 Published online by Cambridge University Press

$$\overline{K} = \left(K + K_P^p + K_P^c\right) = \begin{bmatrix} \overline{k}_{11} & \overline{k}_{12} \\ \overline{k}_{21} & \overline{k}_{22} \end{bmatrix}$$

$$= \begin{bmatrix} k_y + K_{Py}^p + W_y^2 K_{Py}^c & -W_y W_z K_{Py}^c \\ -W_y W_z K_{Pz}^c & k_z + K_{Pz}^p + W_z^2 K_{Pz}^c \end{bmatrix},$$

$$S = \begin{pmatrix} y \\ z \end{pmatrix}, \quad S_d = \begin{pmatrix} y_d \\ z_d \end{pmatrix}, \quad d = \begin{pmatrix} d_y \\ d_z \end{pmatrix} \quad \text{and} \quad F = \begin{pmatrix} F_y \\ F_z \end{pmatrix},$$

$$E = \begin{pmatrix} e_y \\ e_z \end{pmatrix}, \quad E' = \begin{pmatrix} e'_y \\ e'_z \end{pmatrix}, \quad E_c = \begin{pmatrix} e_c \\ e'_c \end{pmatrix},$$

$$P = MS_d'' + CS_d' + KS_d + d,$$

$$\|P\| \le \|M\|\,\|S_d''\| + \|C\|\|S_d'\| + \|K\|\|S_d\| + \|d\| = \|P\|_{\max},$$

$$\lambda_{E'\min} = \min\left(\operatorname{eig}\left\{\overline{K} - \frac{\overline{C}}{2} + \frac{\alpha}{2\beta} I - \frac{K_I^p}{\beta}\right\}\right) > 0,$$

$$\lambda_{E\min} = \min\left(\operatorname{eig}\left\{\left(1 - \frac{\beta}{2}\right)\overline{C} + \frac{\alpha}{2} I - \beta M\right\}\right) > 0,$$

where α and β are user-defined positive constants with $\beta < 1$.

According to the assumptions (A1–A3), it is easy to prove that the parameter $\|P\|_{\max}$ is bounded. For the developed cross-coupled position domain PID controller Eq. (13), we have the following theorem.

3.2. Theorem

A CNC machine system represented in position domain by Eq. (9), where the desired contour shape satisfies assumptions A1 and A2, is controlled by the proposed cross-coupled position domain PID control law in Eq. (13). The contour tracking error and its relative derivative are bounded, and the boundaries are given by

$$\begin{cases} \|E\| \le 2\sqrt{\dfrac{1}{\lambda_{E\min}^2} + \dfrac{1}{\beta\lambda_{E\min}\lambda_{E'\min}}}\, P_{\max} \\ \|E'\| \le 2\sqrt{\dfrac{1}{\lambda_{E'\min}^2} + \dfrac{\beta}{\lambda_{E\min}\lambda_{E'\min}}}\, P_{\max} \end{cases}, \tag{15}$$

provided that the PDC gains and the positive constant parameters for each axis are selected properly, such that

$$\begin{cases} K_{Di}^p > \frac{\alpha}{\beta} + m_i\,\|\ddot{x}\| + c_i\,\|\dot{x}\| + 4\beta m_i\,\|\dot{x}\|^2 \\ K_{Ii}^p < \alpha\beta \\ K_{Pi}^p > \frac{K_{Ii}^p}{\beta} + \frac{K_{Di}^p}{2} + \frac{m_i\|\ddot{x}\| + c_i\|\dot{x}\|}{2} \end{cases} \quad \text{for} \quad i = y,\ z. \tag{16}$$

It is noticed that Eq. (16) provides guidelines about the selection of control gains for the developed position domain PID control.

3.3. Proof of stability

Using the matrix expressions defined in the previous section, the dynamic model Eq. (9) in position domain can be expressed in a matrix form as

$$MS'' + CS' + KS + d = F. \tag{17}$$

https://doi.org/10.1017/S0263574714000769 Published online by Cambridge University Press

The controller in Eq. (13) can be expressed as

$$F = \left(K_P^p + K_P^c\right) E + K_I^p \int_0^x E ds + \left(K_D^p + K_D^c\right) E'. \tag{18}$$

Define

$$\sum (x) = \int_0^x E ds x \quad \text{and} \quad \sum{}' = E. \tag{19}$$

Applying Eqs. (18) and (19) to Eq. (17), the dynamic model can be expressed as functions of contour errors:

$$M E'' + \overline{C} E' + \overline{K} E + K_I^p \Sigma = P. \tag{20}$$

To prove the stability, we define the following three Lyapunov functions:

$$\begin{cases} V_1(E(x), E'(x)) = \frac{1}{2}(E^T \quad E'^T) L_1 \begin{pmatrix} E \\ E' \end{pmatrix} \\ V_2(\Sigma(x), E(x)) = \frac{1}{2}(E^T \quad \Sigma^T) L_2 \begin{pmatrix} E \\ \Sigma \end{pmatrix} \end{cases}, \tag{21}$$

with

$$L_1 = \begin{bmatrix} \overline{K} & \beta M \\ \beta M & M \end{bmatrix} \quad \text{and} \quad L_2 = \begin{bmatrix} \alpha I & K_I^p \\ K_I^p & \beta K_I^p \end{bmatrix},$$

$$V = V_1(\Sigma(x), E(x), E'(x)) + V_2(\Sigma(x), E(x), E'(x)). \tag{22}$$

First, it needs to prove that these three Lyapunov functions (V_1, V_2, and V) are positive definite functions by proving that L_1 are L_2 positive definite.

1. Proof of positive definite of matrices L_1 and V_1.

(a) Positive determinant of matrix $\overline{K}$:
From the definition of control gains, we have

$$k_y + K_{Py}^p + W_y^2 K_{Py}^c > 0.$$

Also, we have

$$\begin{aligned} \det\left(\overline{K}\right) &= \begin{vmatrix} k_y + K_{Py}^p + W_y^2 K_{Py}^c & -W_y W_z K_{Py}^c \\ -W_y W_z K_{Pz}^c & k_z + K_{Pz}^p + W_z^2 K_{Pz}^c \end{vmatrix} \\ &= \left(k_y + K_{Py}^p + W_y^2 K_{Py}^c\right)\left(k_z + K_{Pz}^p\right) + W_z^2 K_{Pz}^c \left(k_y + K_{Py}^p\right) > 0. \end{aligned}$$

Therefore, matrix $\overline{K}$ is positive definite.

(b) Positive determinant of the upper-left 3×3 submatrix of L_1:
As $0 < \beta < 1$, from Eq. (16), we have

$$K_{Py}^p > \frac{1}{2} K_{Dy}^p > 2\beta m_y \|\dot{x}\|^2 > \beta^2 m_y \|\dot{x}\|^2. \tag{23}$$

https://doi.org/10.1017/S0263574714000769 Published online by Cambridge University Press

Based on Eqs. (16) and (23), we have

$$\begin{aligned}
&\left(\overline{k}_{11} - \beta^2 m_y \dot{x}^2\right)\overline{k}_{22} - \overline{k}_{12}\overline{k}_{21} \\
&> \left(k_y + K_{Py}^p + W_y^2 K_{Py}^c - \beta^2 m_y \dot{x}^2\right) W_z^2 K_{Pz}^c - \left(-W_y W_z K_{Py}^c\right)\left(-W_y W_z K_{Pz}^c\right) \\
&> \left(k_y + W_y^2 K_{Py}^c\right) W_z^2 K_{Pz}^c - \left(-W_y W_z K_{Py}^c\right)\left(-W_y W_z K_{Pz}^c\right) \\
&= k_y W_z^2 K_{Pz}^c > 0.
\end{aligned}$$

Therefore, we can prove the determinant of the following 3×3 submatrix of L_1 is positive.

$$\begin{vmatrix} \overline{k}_{11} & \overline{k}_{12} & \beta m_y \dot{x}^2 \\ \overline{k}_{21} & \overline{k}_{22} & 0 \\ \beta m_y \dot{x}^2 & 0 & m_y \dot{x}^2 \end{vmatrix} = \left(\left(\overline{k}_{11} - \beta^2 m_y \dot{x}^2\right)\overline{k}_{22} - \overline{k}_{12}\overline{k}_{21}\right) m_y \dot{x}^2 > 0.$$

(c) Positive determinant of matrix L_1:

$$\begin{aligned}
L_1 &= \begin{vmatrix} \overline{K} & \beta M \\ \beta M & M \end{vmatrix} = \begin{vmatrix} \overline{k}_{11} & \overline{k}_{12} & \beta m_y \dot{x}^2 & 0 \\ \overline{k}_{21} & \overline{k}_{22} & 0 & \beta m_z \dot{x}^2 \\ \beta m_y \dot{x}^2 & 0 & m_y \dot{x}^2 & 0 \\ 0 & \beta m_z \dot{x}^2 & 0 & m_z \dot{x}^2 \end{vmatrix} \\
&= \beta m_z \dot{x}^2 \begin{vmatrix} \overline{k}_{11} & \beta m_y \dot{x}^2 & 0 \\ \overline{k}_{21} & 0 & \beta m_z \dot{x}^2 \\ \beta m_y \dot{x}^2 & m_y \dot{x}^2 & 0 \end{vmatrix} + m_z \dot{x}^2 \begin{vmatrix} \overline{k}_{11} & \overline{k}_{12} & \beta m_y \dot{x}^2 \\ \overline{k}_{21} & \overline{k}_{22} & 0 \\ \beta m_y \dot{x}^2 & 0 & m_y \dot{x}^2 \end{vmatrix} \\
&= m_y m_z \dot{x}^4 \left(\beta^4 m_y m_z \dot{x}^4 + \frac{1}{2}\left(\overline{k}_{11}\left(\overline{k}_{22} - 2\beta^2 m_z \dot{x}^2\right) - \overline{k}_{12}\overline{k}_{21}\right) \right. \\
&\quad \left. + \frac{1}{2}\left(\overline{k}_{22}\left(\overline{k}_{11} - 2\beta^2 m_y \dot{x}^2\right) - \overline{k}_{12}\overline{k}_{21}\right) \right).
\end{aligned}$$

From Eq. (16), considering $\beta < 1$, we have

$$\begin{cases} K_{Py}^p > \dfrac{K_{Di}^2}{2} > 2\beta m_y \|\dot{x}\|^2 > 2\beta^2 m_y \|\dot{x}\|^2 \\ K_{Pz}^p > \dfrac{K_{Di}^2}{2} > 2\beta m_z \|\dot{x}\|^2 > 2\beta^2 m_z \|\dot{x}\|^2 \end{cases}. \tag{24}$$

Based on Eq. (24), we can demonstrate that

$$\begin{cases} \overline{k}_{11}\left(\overline{k}_{22} - 2\beta^2 m_z \dot{x}^2\right) - \overline{k}_{12}\overline{k}_{21} > 0 \\ \overline{k}_{22}\left(\overline{k}_{11} - 2\beta^2 m_y \dot{x}^2\right) - \overline{k}_{12}\overline{k}_{21} > 0 \end{cases}.$$

Therefore, the determinant of $\begin{vmatrix} \overline{K} & \beta M \\ \beta M & M \end{vmatrix}$ is also positive.

As all the determinants associated with all upper-left submatrices of L_1 are positive, according to Sylvester's criterion, we prove that L_1 is a positive definite matrix and V_1 is a positive definite function.

2. Proof of positive definite of matrix L_2 and V_2.

https://doi.org/10.1017/S0263574714000769 Published online by Cambridge University Press

From the definition, we have

$$L_2 = \begin{bmatrix} \alpha I & K_I^p \\ K_I^p & \beta K_I^p \end{bmatrix} = \begin{bmatrix} \alpha & 0 & K_{Iy}^p & 0 \\ 0 & \alpha & 0 & K_{Iz}^p \\ K_{Iy}^p & 0 & \beta K_{Iy}^p & 0 \\ 0 & K_{Iz}^p & 0 & \beta K_{Iz}^p \end{bmatrix}.$$

According to Eq. (16), it is easy to prove that the first two upper-left 1×1 and 2×2 submatrices of L_2 are positive as:

$$\alpha > 0 \quad \text{and} \quad \alpha^2 > 0$$

Also, according to Eq. (16), it can be demonstrated that the determinant of the upper-left 3×3 submatrix of L_2 is positive as

$$\begin{vmatrix} \alpha & 0 & K_{Iy}^p \\ 0 & \alpha & 0 \\ K_{Iy}^p & 0 & \beta K_{Iy}^p \end{vmatrix} = \alpha K_{Iy}^p \left(\alpha\beta - K_{Iy}^p\right) > 0.$$

Finally, we calculate the determinant of matrix L_2 as follows:

$$\begin{aligned} L_2 &= \begin{vmatrix} \alpha & 0 & K_{Iy}^p & 0 \\ 0 & \alpha & 0 & K_{Iz}^p \\ K_{Iy}^p & 0 & \beta K_{Iy}^p & 0 \\ 0 & K_{Iz}^p & 0 & \beta K_{Iz}^p \end{vmatrix} = \beta K_{Iz}^p \begin{vmatrix} \alpha & 0 & K_{Iy}^p \\ 0 & \alpha & 0 \\ K_{Iy}^p & 0 & \beta K_{Iy}^p \end{vmatrix} + K_{Iz}^p \begin{vmatrix} \alpha & K_{Iy}^p & 0 \\ 0 & 0 & K_{Iz}^p \\ K_{Iy}^p & \beta K_{Iy}^p & 0 \end{vmatrix} \\ &> K_{Iy}^p K_{Iz}^p \left(K_{Iy}^p - \alpha\beta\right)\left(K_{Iz}^p - \alpha\beta\right). \end{aligned}$$

From Eq. (16), we have

$$\alpha\beta > K_{Iy}^p \quad \text{and} \quad \alpha\beta > K_{Iz}^p. \tag{25}$$

Using Eq. (25), we prove that the determinant of matrix L_2 is positive.

As all the determinants associated with all upper-left submatrices of L_2 are positive, we prove that L_2 is a positive definite matrix and V_2 is a positive definite function.

As V_1 and V_2 are positive definite, it concludes that the Lyapunov function V in Eq. (22) is also positive definite.

3. Preparation for the proof of the negativity of function V'.

Taking the derivative of V in Eq. (22) and considering Eq. (21), we have

$$\begin{aligned} V' &= \begin{pmatrix} E'^T & E''^T \end{pmatrix} \begin{bmatrix} K_P & \beta M \\ \beta M & M \end{bmatrix} \begin{pmatrix} E \\ E' \end{pmatrix} \\ &= E'^T K_P E + \left(E'^T + \beta E^T\right) M E'' + \beta E'^T M E'. \end{aligned} \tag{26}$$

Applying Eq. (20) to Eq. (26), the following equation can be obtained:

$$\begin{aligned} V' &= E'^T \left(\overline{K} + \alpha I\right) E + \beta E'^T M E' + E^T K_I^p E + \left(E'^T + \beta E^T\right) K_I^p \Sigma \\ &\quad + \left(E'^T + \beta E^T\right)\left(P - \left(\overline{C} E' + \overline{K} E + K_I^p \Sigma\right)\right) \\ &= -E'^T(\overline{C} - \beta M)E' - E^T \left(\beta \overline{K} - K_I^p\right) E - E^T(\beta \overline{C} - \alpha I)E' + (E'^T + \beta E^T)P. \end{aligned} \tag{27}$$

In the following sections, we first demonstrate that the three matrices in Eq. (27) are positive definite, then we prove the positive definite of two combined matrices, and finally, we conclude the negative definite of function V'.

https://doi.org/10.1017/S0263574714000769 Published online by Cambridge University Press

3.1. Proof of positive definite of the following three matrices:

$$\overline{C} - \beta M = \begin{bmatrix} (1-\beta)\, m_y \ddot{x} + c_y \dot{x} + K_{Dy}^p + W_y^2 K_{Dy}^c & -W_y W_z K_{Dy}^c \\ -W_y W_z K_{Dz}^c & (1-\beta)\, m_z \ddot{x} + c_z \dot{x} + K_{Dz}^p + W_z^2 K_{Dz}^c \end{bmatrix},$$

$$\beta \overline{K} - K_I^P = \beta \begin{bmatrix} k_y + K_{Py}^p + W_y^2 K_{Py}^c - K_{Iy}^p/\beta & -W_y W_z K_{Py}^c \\ -W_y W_z K_{Pz}^c & k_z + K_{Pz}^p + W_z^2 K_{Pz}^c - K_{Iz}^p/\beta \end{bmatrix},$$

$$\beta \overline{C} - \alpha I = \beta \begin{bmatrix} m_y \ddot{x} + c_y \dot{x} + K_{Dy}^p + W_y^2 K_{Dy}^c - \alpha/\beta & -W_y W_z K_{Dy}^c \\ -W_y W_z K_{Dz}^c & m_z \ddot{x} + c_z \dot{x} + K_{Dz}^p + W_z^2 K_{Dz}^c - \alpha/\beta \end{bmatrix}.$$

(a) Positivity of matrix $\overline{C} - \beta M$:
From Eq. (16), we have

$$\begin{cases} K_{Dy}^p > m_y \|\ddot{x}\| + c_y \|\dot{x}\| > (1-\beta)\, m_y \|\ddot{x}\| + c_y \|\dot{x}\| \\ K_{Dz}^p > m_z \|\ddot{x}\| + c_z \|\dot{x}\| > (1-\beta)\, m_z \|\ddot{x}\| + c_z \|\dot{x}\| \end{cases}. \tag{28}$$

Based on Eq. (28), we have

$$\begin{cases} (1-\beta)\, m_y \ddot{x} + c_y \dot{x} + K_{Dy}^p + W_y^2 K_{Dy}^c > W_y^2 K_{Dy}^c > 0 \\ (1-\beta)\, m_z \ddot{x} + c_z \dot{x} + K_{Dz}^p + W_z^2 K_{Dz}^c > W_z^2 K_{Dz}^c > 0 \end{cases}. \tag{29}$$

Therefore, the upper-left submatrix of $\overline{C} - \beta M$ is positive.
Also, the determinant of matrix $\overline{C} - \beta M$is

$$\begin{aligned} \left|\overline{C} - \beta M\right| &= \left((1-\beta)\, m_y \ddot{x} + c_y \dot{x} + K_{Dy}^p + W_y^2 K_{Dy}^c\right)\left((1-\beta)\, m_z \ddot{x} + c_z \dot{x} + K_{Dz}^p + W_z^2 K_{Dz}^c\right) \\ &\quad - W_y^2 W_z^2 K_{Dy}^c K_{Dz}^c \\ &> W_y^2 K_{Dy}^c W_z^2 K_{Dz}^c - W_y^2 W_z^2 K_{Dy}^c K_{Dz}^c = 0. \end{aligned}$$

Therefore, we prove that $\overline{C} - \beta M$ is positive definite.

(b) Positivity of matrix $\beta \overline{K} - K_I^P$:
Similarly, from Eq. (16), we have

$$\beta K_{Py}^p > K_{Iy}^p \quad \text{and} \quad \beta K_{Pz}^p > K_{Iz}^p. \tag{30}$$

It concludes that the determinant of the upper-left submatrix of $\beta \overline{K} - K_I^P$ is positive.
Also, we get the determinant of $\beta \overline{K} - K_I^P$ as follows:

$$\begin{aligned} \left|\beta \overline{K} - K_I^P\right| &= \beta\left(k_y + K_{Py}^p + W_y^2 K_{Py}^c - K_{Iy}^p/\beta\right)\left(k_z + K_{Pz}^p + W_z^2 K_{Pz}^c - K_{Iz}^p/\beta\right) \\ &\quad - \beta W_y^2 W_z^2 K_{Py}^c K_{Pz}^c > \beta\left(k_y + W_y^2 K_{Py}^c\right)\left(k_z + W_z^2 K_{Pz}^c\right) - \beta W_y^2 W_z^2 K_{Py}^c K_{Pz}^c > 0. \end{aligned}$$

Therefore we prove that $\beta \overline{K} - K_I^P$ is positive definite.

(c) Positivity of matrix $\beta \overline{C} - \alpha I$:
Based on Eq. (16), we have

$$\begin{cases} K_{Dy}^p > \alpha/\beta + m_y \|\ddot{x}\| + c_y \|\dot{x}\| \\ K_{Dz}^p > \alpha/\beta + m_z \|\ddot{x}\| + c_z \|\dot{x}\| \end{cases}. \tag{31}$$

We demonstrate that the determinant of the upper-left submatrix of $\beta \overline{C} - \alpha I$ is positive.

https://doi.org/10.1017/S0263574714000769 Published online by Cambridge University Press

We calculate the determinant of matrix $\beta\overline{C} - \alpha I$ as follows:

$$\begin{aligned}\left|\beta\overline{C} - \alpha I\right| &= \beta\left(m_y\ddot{x} + c_y\dot{x} + K_{Dy}^p + W_y^2 K_{Dy}^c - \alpha/\beta\right)\left(m_z\ddot{x} + c_z\dot{x} + K_{Dz}^p + W_z^2 K_{Dz}^c - \alpha/\beta\right) \\ &\quad - \beta W_y^2 W_z^2 K_{Dy}^c K_{Dz}^c \\ &> \beta\left(W_y^2 K_{Dy}^c\right)\left(W_z^2 K_{Dz}^c\right) - \beta W_y^2 W_z^2 K_{Dy}^c K_{Dz}^c = 0.\end{aligned}$$

Therefore, we prove that $\beta\overline{C} - \alpha I$ is positive definite.
As $\beta\overline{C} - \alpha I$ is positive definite, the following function holds:

$$\begin{pmatrix} E'^T & E \end{pmatrix}\begin{bmatrix} \beta\overline{C} - \alpha I & \beta\overline{C} - \alpha I \\ \beta\overline{C} - \alpha I & \beta\overline{C} - \alpha I \end{bmatrix}\begin{pmatrix} E' \\ E \end{pmatrix} \geq 0. \tag{32}$$

Expanding Eq. (32), we can obtain the following inequality:

$$-E^T\left(\beta\overline{C} - \alpha I\right)E' \leq \frac{1}{2}(E^T(\beta\overline{C} - \alpha I)E + E'^T(\beta\overline{C} - \alpha I)E'). \tag{33}$$

Applying Eqs. (33) to Eq. (27), it can be shown that

$$\begin{aligned}V' \leq &-E'^T\left(\left(1 - \frac{\beta}{2}\right)\overline{C} + \frac{\alpha}{2}I - \beta M\right)E' - \beta E^T\left(\overline{K} - \frac{\overline{C}}{2} + \frac{\alpha}{2\beta}I - \frac{K_I^p}{\beta}\right)E \\ &+ \left(E'^T + \beta E^T\right)P.\end{aligned} \tag{34}$$

3.2 Proof of positive definite of the above two matrices in Eq. (34):

(a) Positivity of matrix $\left(1 - \frac{\beta}{2}\right)\overline{C} + \frac{\alpha}{2}I - \beta M$:
From the notations defined before, we have

$$\begin{aligned}&\left(1 - \frac{\beta}{2}\right)\overline{C} + \frac{\alpha}{2}I - \beta M \\ &= \left(1 - \frac{\beta}{2}\right)\begin{bmatrix} m_y\ddot{x} + c_y\dot{x} + K_{Dy}^p + W_y^2 K_{Dy}^c & -W_y W_z K_{Dy}^c \\ -W_y W_z K_{Dz}^c & m_z\ddot{x} + c_z\dot{x} + K_{Dz}^p + W_z^2 K_{Dz}^c \end{bmatrix} \\ &\quad + \begin{bmatrix} \frac{\alpha}{2} - \beta m_y\dot{x}^2 & 0 \\ 0 & \frac{\alpha}{2} - \beta m_z\dot{x}^2 \end{bmatrix}.\end{aligned}$$

According to Eq. (16), we have

$$\begin{cases} K_{Dy}^p > \alpha/\beta + m_y\left\|\ddot{x}\right\| + c_y\left\|\dot{x}\right\| + 4\beta m_y\left\|\dot{x}\right\|^2 \\ K_{Dz}^p > \alpha/\beta + m_z\left\|\ddot{x}\right\| + c_z\left\|\dot{x}\right\| + 4\beta m_z\left\|\dot{x}\right\|^2 \end{cases}. \tag{35}$$

https://doi.org/10.1017/S0263574714000769 Published online by Cambridge University Press

From Eq. (35), we have

$$\begin{aligned}
&\left(1-\frac{\beta}{2}\right)\left(m_y\ddot{x}+c_y\dot{x}+K_{Dy}^{p}\right)+\frac{\alpha}{2}\\
&> \frac{\alpha}{\beta}\left(1-\frac{\beta}{2}\right)+\frac{\alpha}{2}+\left(1-\frac{\beta}{2}\right)\left(m_y\left(\ddot{x}+\|\ddot{x}\|\right)+c_y\left(\dot{x}+\|\dot{x}\|\right)+4\beta m_y\|\dot{x}\|^2\right)\\
&> \left(1-\frac{\beta}{2}\right)\left(m_y\left(\ddot{x}+\|\ddot{x}\|\right)+c_y\left(\dot{x}+\|\dot{x}\|\right)+4\beta m_y\|\dot{x}\|^2\right)\\
&> (4-2\beta)\,\beta m_y\|\dot{x}\|^2\\
&> \beta m_y\dot{x}^2.
\end{aligned}$$

Therefore, we prove that

$$\begin{cases}\left(1-\frac{\beta}{2}\right)\left(m_y\ddot{x}+c_y\dot{x}+K_{Dy}^{p}++W_y^2K_{Dy}^{c}\right)+\frac{\alpha}{2}>\beta m_y\dot{x}^2\\ \left(1-\frac{\beta}{2}\right)\left(m_z\ddot{x}+c_z\dot{x}+K_{Dz}^{p}++W_z^2K_{Dz}^{c}\right)+\frac{\alpha}{2}>\beta m_z\dot{x}^2\end{cases}.$$

Also, we prove the positive determinant of $(1-\frac{\beta}{2})\overline{C}+\frac{\alpha}{2}I-\beta M$:

$$\begin{aligned}
&\det\left(\left(1-\frac{\beta}{2}\right)\overline{C}+\frac{\alpha}{2}I-\beta M\right)\\
&>\left(\left(1-\frac{\beta}{2}\right)\left(m_y\ddot{x}+c_y\dot{x}+K_{Dy}^{p}++W_y^2K_{Dy}^{c}\right)+\frac{\alpha}{2}-\beta m_y\dot{x}^2\right)\\
&\times\left(\left(1-\frac{\beta}{2}\right)\left(m_z\ddot{x}+c_z\dot{x}+K_{Dz}^{p}++W_z^2K_{Dz}^{c}\right)+\frac{\alpha}{2}-\beta m_z\dot{x}^2\right)>0.
\end{aligned}$$

Therefore, we demonstrate that $(1-\frac{\beta}{2})\overline{C}+\frac{\alpha}{2}I-\beta M$is positive definite.
We define the minimum eigenvalue of matrix $(1-\frac{\beta}{2})\overline{C}+\frac{\alpha}{2}I-\beta M$ as $\lambda_{E'\min}$ (>0); then we have

$$-E'^{T}\left(\left(1-\frac{\beta}{2}\right)\overline{C}+\frac{\alpha}{2}I-\beta M\right)E'\le-\lambda_{E'\min}\|E'\|^2. \tag{36}$$

(b) The positive determinant of $\overline{K}-\frac{\overline{C}}{2}+\frac{\alpha}{2\beta}I-\frac{K_I^p}{\beta}$:
Based on Eq. (16), we have

$$\begin{cases}k_y+K_{Py}^{p}+\dfrac{\alpha}{2\beta}>\dfrac{m_y\ddot{x}+c_y\dot{x}+K_{Dy}^{p}}{2}+\dfrac{K_{Iy}^{p}}{\beta}\\ k_z+K_{Pz}^{p}+\dfrac{\alpha}{2\beta}>\dfrac{m_z\ddot{x}+c_z\dot{x}+K_{Dz}^{p}}{2}+\dfrac{K_{Iz}^{p}}{\beta}\end{cases}$$

$$\begin{aligned}
&\det\left(\overline{K}-\frac{\overline{C}}{2}+\frac{\alpha}{2\beta}I-\frac{K_I^p}{\beta}\right)>\left(k_y+K_{Py}^{p}+\frac{\alpha}{2\beta}-\frac{m_y\ddot{x}+c_y\dot{x}+K_{Dy}^{p}}{2}-\frac{K_{Iy}^{p}}{\beta}\right)\\
&\times\left(k_z+K_{Pz}^{p}+\frac{\alpha}{2\beta}-\frac{m_z\ddot{x}+c_z\dot{x}+K_{Dz}^{p}}{2}-\frac{K_{Iz}^{p}}{\beta}\right)>0.
\end{aligned}$$

https://doi.org/10.1017/S0263574714000769 Published online by Cambridge University Press

Therefore, we demonstrate that matrix $\overline{K} - \frac{\overline{C}}{2} + \frac{\alpha}{2\beta} I - \frac{K_I^p}{\beta}$ is also positive definite.

If we define the minimum eigenvalue of matrix $\overline{K} - \frac{\overline{C}}{2} + \frac{\alpha}{2\beta} I - \frac{K_I^p}{\beta}$ as $\lambda_{E\min}$ (> 0), then we have

$$-\beta E^T \left(\overline{K} - \frac{\overline{C}}{2} + \frac{\alpha}{2\beta} I - \frac{K_I^p}{\beta} \right) E \leq -\beta \lambda_{E\min} \|E\|^2 . \tag{37}$$

4. System stability with bounded tracking error.

Applying Eqs. (36) and (37) to Eq. (34), the following inequality holds:

$$V' \leq -\lambda_{E'\min} \|E'\|^2 - \beta \lambda_{E\min} \|E\|^2 + \|E'\| P_{\max} + \beta \|E\| P_{\max}. \tag{38}$$

We have the following inequality:

$$az - bz^2 \leq \frac{a^2}{b} - \frac{1}{4} bz^2 \quad \forall \quad a > 0, \quad b > 0.$$

Applying the above inequality to Eq. (38), we have

$$V' \leq -\frac{\lambda_{E'\min}}{4} \|E'\|^2 - \frac{\beta \lambda_{E\min}}{4} \|E\|^2 + \left(\frac{1}{\lambda_{E'\min}} + \frac{\beta}{\lambda_{E\min}} \right) P_{\max}^2. \tag{39}$$

From Eq. (39), it immediately follows that

$$V' < 0, \qquad \forall \quad \|E\| > \delta_E = 2\sqrt{\frac{1}{\lambda_{E\min}^2} + \frac{1}{\beta \lambda_{E\min} \lambda_{E'\min}}} P_{\max}$$

$$\text{or} \quad \|E'\| > \delta_E' = 2\sqrt{\frac{1}{\lambda_{E'\min}^2} + \frac{\beta}{\lambda_{E\min} \lambda_{E'\min}}} P_{\max}.$$

In other words, the derivative of V with respect to the master motion is negative outside of the compact set (bound) B$= \{\|E < \delta_E\|, \quad \|E' < \delta_E'\|\}$. Based on the Lyapunov theorem,[16,17] we conclude that the system controlled by the PDC/CCC is globally ultimately bounded.

The boundaries for both the tracking error and the relative derivative of the tracking error are obtained as follows:

$$\begin{cases} \|E\| \leq 2\sqrt{\dfrac{1}{\lambda_{E\min}^2} + \dfrac{1}{\beta \lambda_{E\min} \lambda_{E'\min}}} P_{\max} \\ \|E'\| \leq 2\sqrt{\dfrac{1}{\lambda_{E'\min}^2} + \dfrac{\beta}{\lambda_{E\min} \lambda_{E'\min}}} P_{\max} \end{cases} . \tag{40}$$

From Eq. (40), it concludes that the two eigenvalues determine the bounds of the contour errors for a specified contour where $P_{\max}$ is constant and fixed. From Eq. (36) and the definition of $\lambda_{E'\min}$, one can see that a larger control gain K_{Di}^p will increase $\lambda_{E'\min}$, while a larger control gain K_{Pi}^p will increase $\lambda_{E\min}$ according to Eq. (37) and the definition of $\lambda_{E\min}$. Increasing both gains will reduce the contour error bounds from Eq. (40). Such a conclusion is very similar with a PID control in time domain and will be verified in the next section. It also needs to mention that the cross-coupled gains do not affect the stability of the proposed PDC law. Therefore, the selection of cross-coupled gains is free.

https://doi.org/10.1017/S0263574714000769 Published online by Cambridge University Press

Table I. System parameters.

Axis	X	Y	Z
Mass (m_i [kg])	15	10	5
Damping (c_i [Ns/m])	7	7	7
Spring constant (k_i [N/m])	50	50	50

Table II. Initial and final axial positions for zigzag and diamond contours.

	Segment 1		Segment 2		Segment 3		Segment 4	
	p_i (m)	p_f (m)	p_i (m)	p_f (m)	p_i (m)	p_f (m)	p_i (m)	p_f (m)
Zigzag contour								
X-axis	−4	−2	−2	0	0	2	2	4
Y-axis	−4	−2	−2	0	0	2	2	4
Z-axis	0	2	2	0	0	2	2	0
Diamond contour								
X-axis	−2	0	0	2	2	0	0	−2
Y-axis	−2	0	0	2	2	0	0	−2
Z-axis	0	2	2	0	0	−2	−2	0

4. Simulation Case Study

4.1. Simulation setup

It is assumed that the three-axis CNC system has the following system parameters listed in Table I.

In the simulations, the disturbances are assumed as the following uniformly distributed random numbers:

$$d = \begin{bmatrix} d_1 \\ d_2 \\ d_3 \end{bmatrix} = \begin{bmatrix} 4 \times \text{rand}(\,) \\ 4 \times \text{rand}(\,) \\ 4 \times \text{rand}(\,) \end{bmatrix} \quad \text{(N)},$$

where rand( ) will produce pseudorandom values drawn from the standard uniform distribution on the open interval (0,1). The introduced disturbance can be viewed as the combination of random noise (with zero mean) and a system bias (positive). In addition, different levels of disturbances are considered to demonstrate the effectiveness of the proposed controller.

Both the linear and circular motions were simulated for TDC, TDC/CCC, PDC, and PDC/CCC controllers. The desired three different contours are shown in Fig. 3.

To ensure a smooth motion, a high-order polynomial ($r(t)$) is used to generate the linear trajectories of each segment in each axis for time domain PID control, where T is the total time duration for a trajectory.

$$\begin{cases} q(t) = \left(p_f - p_i\right) r(t) + p_i \\ r(t) = 10\left(\dfrac{t}{T}\right)^3 - 15\left(\dfrac{t}{T}\right)^4 + 5\left(\dfrac{t}{T}\right)^5 \end{cases},$$

where p_f and p_i are the final and initial positions of each segment, respectively. For zigzag and diamond contours shown in Fig. 2, the values of the final and initial positions are listed in Table II.

4.2. Linear motion contour tracking

In all linear motion simulations, $T = 40$ s, and the PID control gains in time domain for all three axes are set as: $K_{Pi}^t = 80,000$, $K_{Ii}^t = 50,000$, and $K_{Di}^t = 70,000$. The same PID gains are applied to the PDC controllers ($K_{Pi}^p = 80,000$, $K_{Ii}^p = 50,000$, and $K_{Di}^p = 70,000$) that can satisfy Eq. (16). For the master motion, the same time domain PID control is applied to the X-axis motion. Also, the CCC gains are set as: $K_{Pi}^c = 16,000$ and $K_{Di}^c = 14,000$. The sampling rate of the TDC is 2000 Hz and the equidistant measurement displacement in the master motion for the PDC is 0.0001 m.

https://doi.org/10.1017/S0263574714000769 Published online by Cambridge University Press

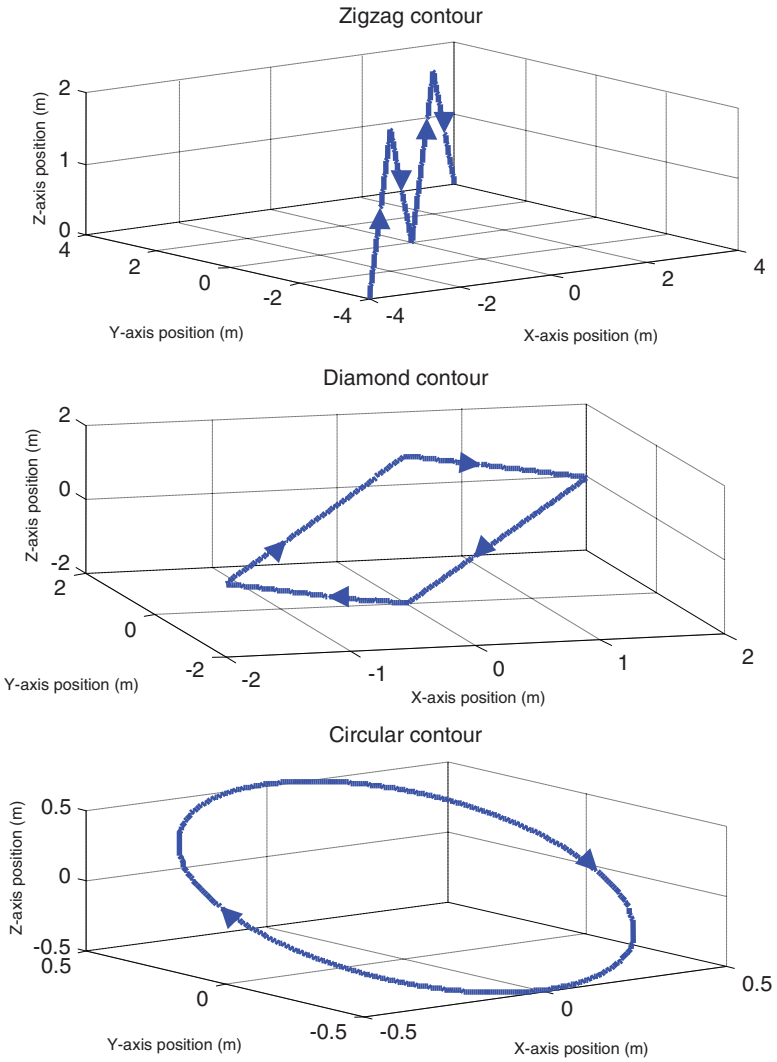


Fig. 3. Desired linear and circular contours.

Remark 4. To achieve good tracking performance, it is common knowledge that large control gains are required for fast motion under PID control compared to a slow motion control. For all test cases, the average speeds in time domain are less than the relative derivatives in the position domain. In all the simulations, we choose the same control gains for both TDC and PDC and compare contour performances. Indeed, the PDC controllers are under disadvantage conditions compared with TDC under the same control gains condition. But the PDC still obtains better contour performances as being shown in simulation results.

Tracking errors for the zigzag motion controlled by TDC and PDC controllers are displayed in Fig. 4 and tracking errors for the diamond motion are shown in Fig. 5. Using the selected control gains, for the zigzag contour tracking shown in Fig. 4, the absolutely maximum tracking error based on the TDC controller is approximately 2.5×10^{-3} m for the X and Y axes because of their identical motions with slightly different disturbances, while it is about 1.7×10^{-3} for the Z-axis. Such a result is expected because of the half motion range in the Z-axis compared to the X and Y motions and the same control gains used for all three axes. On the other hand, for the PDC and PDC with CCC (PDC/CCC for short), the tracking performances are much better than the counterparts in time domain, with less than half tracking errors for all axes.

A similar conclusion is drawn for the diamond contour tracking control as shown in Fig. 5. In Fig. 5, the arrows show the master motion direction for all position domain controllers. More accurate tracking performance was also achieved by PDC as errors in the slave axes are smaller than that of

https://doi.org/10.1017/S0263574714000769 Published online by Cambridge University Press

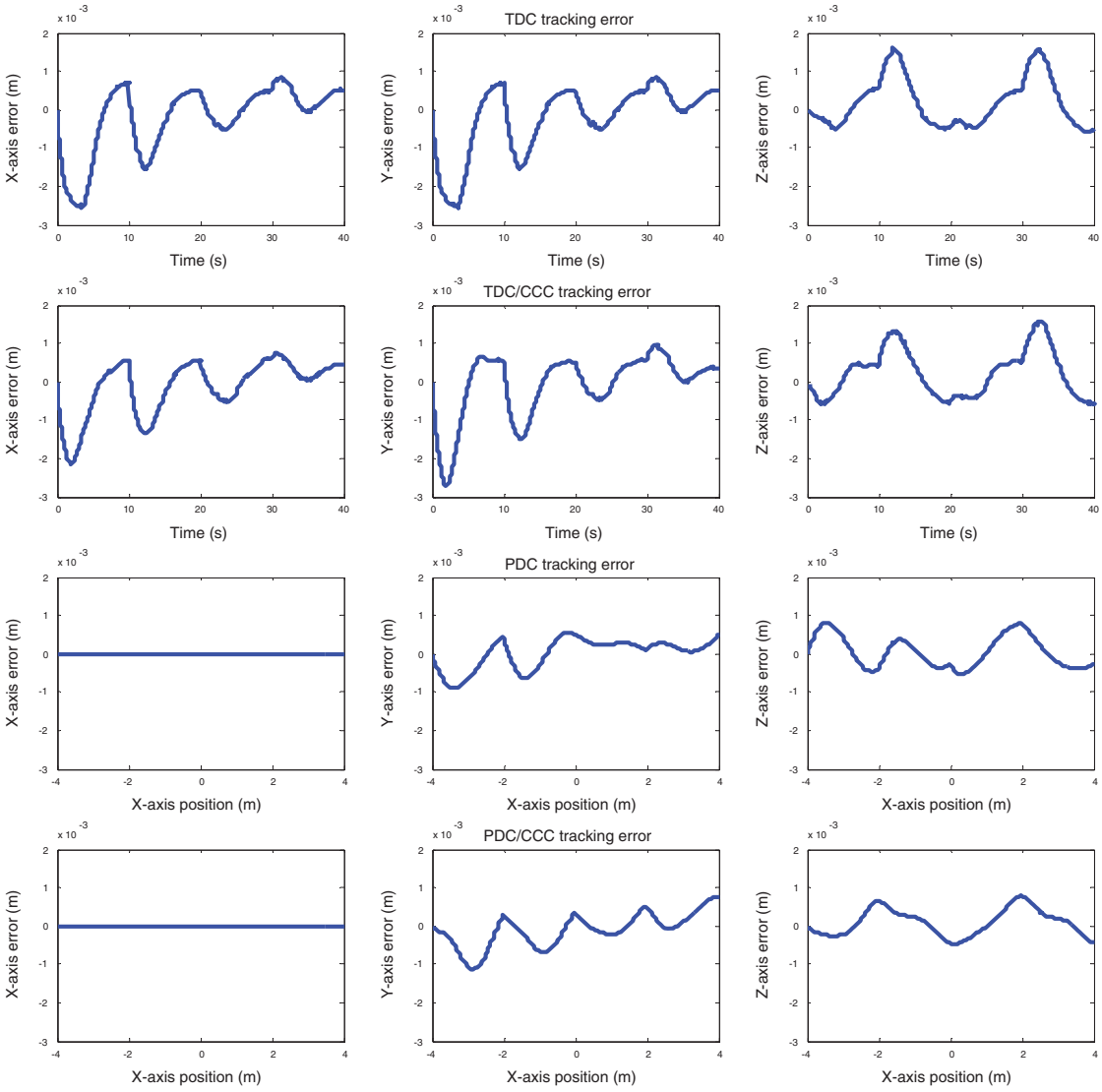


Fig. 4. Axial position tracking error of zigzag contour under four different controllers.

the TDC controller. It is also shown that PDC/CCC obtained highly improved tracking performance over both the PDC and TDC controllers. Another point to note from the plots of the tracking error is that there is no tracking error in the X-axis for both PDC and PDC/CCC controllers because the X-axis is used as a reference.

Figure 6 displays the contour tracking error plots obtained by each controller for both zigzag and diamond motions. It is observed that both PDC and PDC/CCC get lower contour tracking errors throughout entire motions in comparison to the TDC counterparts. For both zigzag and diamond contours, the PDC/CCC obtained the lowest contour tracking errors throughout the motion with maximum contouring errors of around 1.0×10^{-3} m for both zigzag and diamond motions.

The statistics of contour tracking performances of each controller are listed in Table III based on 10 simulation results, because of the introduction of the random disturbance in the dynamic model. The data shown in all following tables are used to evaluate the contour tracking performances controlled by different methods under different situations. The overall performance index, which includes the mean and standard deviation (S.D.) for all contour errors over 10 different simulations, is used to measure the overall contour error for a specific contour, the maximum contour error index, which includes the mean and S.D. of the maximum contour errors from these 10 simulations, is used to measure the maximum contour tracking error and distribution. From Table III, one can see that the overall performance index and maximum contour error index for both PDC controllers are better

https://doi.org/10.1017/S0263574714000769 Published online by Cambridge University Press

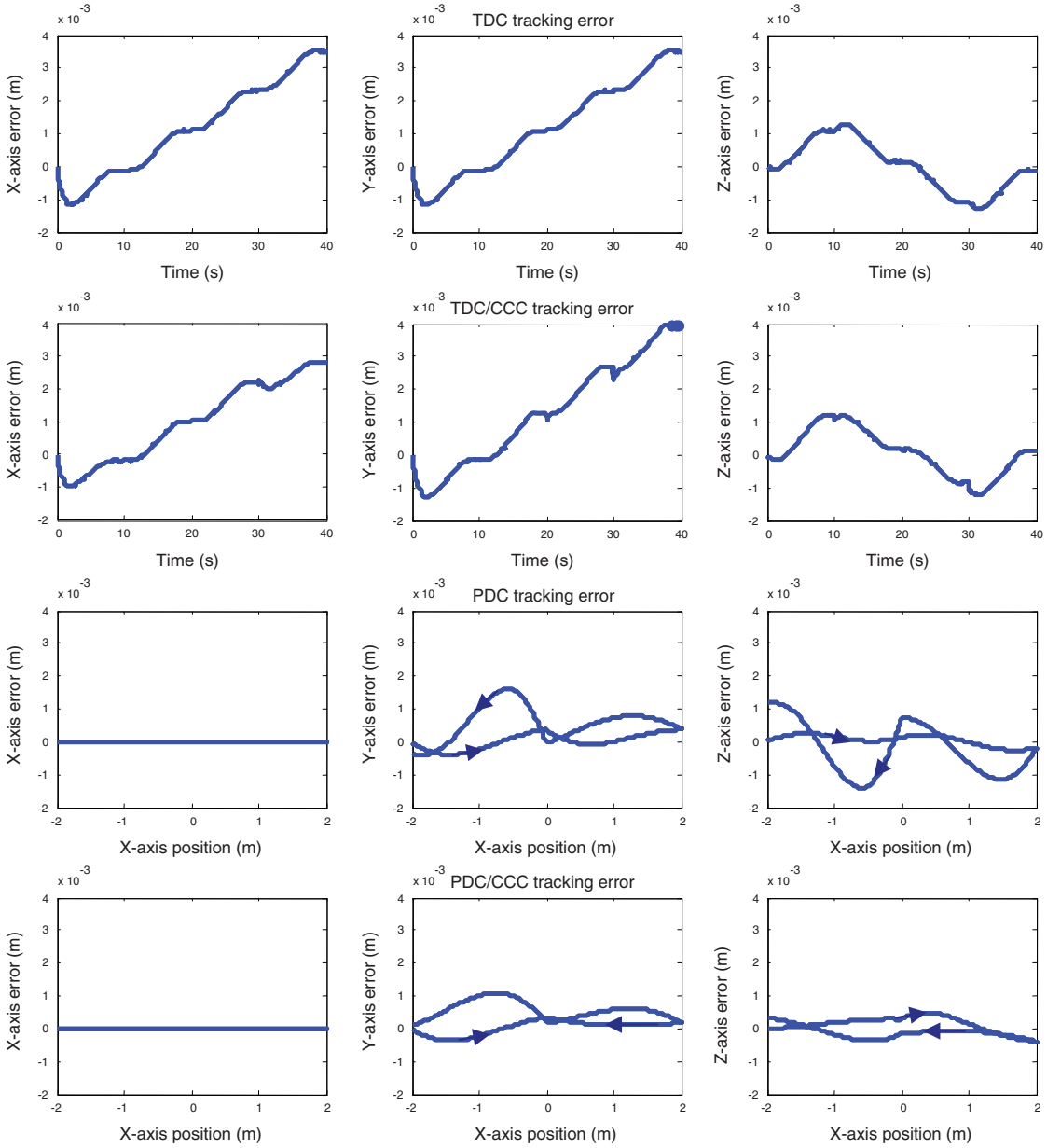


Fig. 5. Axial position tracking errors of diamond contour under four different controllers.

than those in TDC controllers. It is also shown that a considerable improvement in contour tracking was achieved by the PDC/CCC as the overall performance index and maximum error index are significantly low (around quarter to half) compared to that of the TDC controllers. The PDC/CCC is slightly better than the PDC without CCC, as smaller performance indexes are obtained.

To examine the effect of control gains and the effect of different levels of disturbances on contour tracking performances, high control gains (doubled values) are used and large random disturbances (doubled magnitudes) are applied for contour tracking control of the diamond motion. The contour tracking performance indexes are listed in Table IV.

Compared with Table III of the diamond contour tracking, it can be found that large control gains can reduce the contour errors for all the control methods. In terms of the reduction of maximum contour error and the overall contour errors, the PDC/CCC is still the best control that reduced the values of indexes about 50% compared to the low control gain case. For the case where high level of disturbance is introduced, the contour tracking performance indexes, listed in Table IV of the doubled

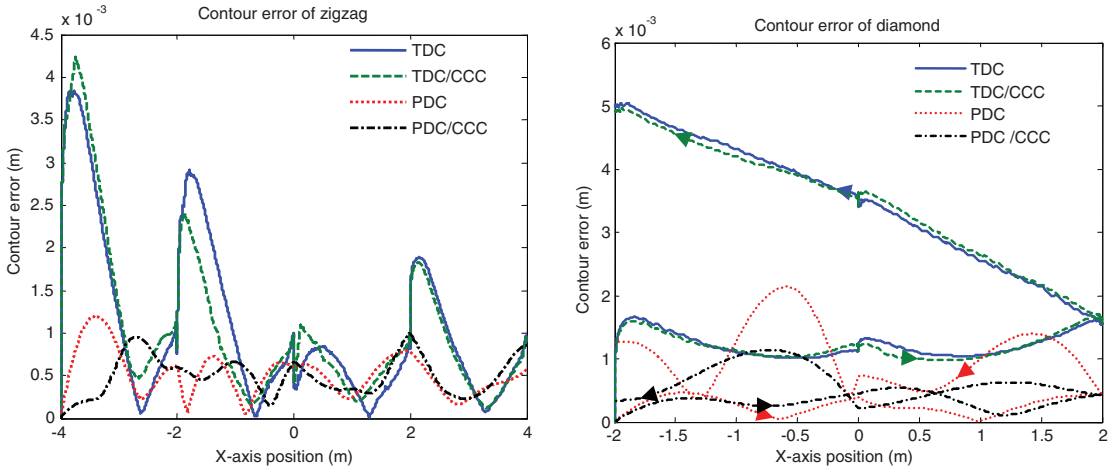
https://doi.org/10.1017/S0263574714000769 Published online by Cambridge University Press

Table III. Contour tracking performance for zigzag and diamond motions ($\times 10^{-3}$ m).

	Zigzag motion				Diamond motion			
	Overall		Maximum		Overall		Maximum	
Controllers	Mean	S.D.	Mean	S.D.	Mean	S.D.	Mean	S.D.
TDC	1.211	0.946	3.983	0.203	2.335	1.345	5.064	4.41E-3
TDC/CCC	1.125	0.830	3.698	0.331	2.334	1.327	4.958	8.33E-3
PDC	0.516	0.249	1.201	0.005	0.656	0.531	2.127	5.31E-3
PDC/CCC	0.492	0.245	1.087	0.067	0.474	0.253	1.140	7.48E-4

Table IV. Contour tracking performance index for diamond motion with doubled control gains/double disturbances ($\times$ 10^{-3} m).

	Doubled control gains				Doubled disturbances			
	Overall		Maximum		Overall		Maximum	
Controllers	Mean	S.D.	Mean	S.D.	Mean	S.D.	Mean	S.D.
TDC	0.796	0.597	2.337	9.999E-2	2.349	1.352	5.086	8.16E-4
TDC/CCC	0.813	0.534	2.353	0.206	2.357	1.334	4.976	9.80E-3
PDC	0.259	0.127	0.682	3.537E-2	0.648	0.521	2.107	2.16E-3
PDC/CCC	0.235	0.133	0.603	4.031E-3	0.475	0.254	1.144	1.41E-3



(a) Zigzag contour error.

(b) Diamond contour error.

Fig. 6. Contour errors of linear motions under four different controllers.

disturbance case, are almost the same as the low-level case shown in Table III of the diamond motion. Such results demonstrate the robustness of the controllers to deal with the random disturbances.

For the contour plots of the diamond contour motion shown in Fig. 7, the tracking errors have been magnified by a factor of 100. It is shown that TDC controllers resulted in larger contouring errors in comparison to both PDC controllers. The contour errors of the TDC controllers are observed to increase at a large rate from segment to segment in comparison to the PDC controllers. This is the result where all axial tracking errors contribute to the contouring error for the TDC controller. With the PDC controller, only the slave axes (Y-axis and Z-axis) tracking errors contribute to the total contouring errors as there is no tracking error for the reference X-axis, and this results in a small contouring error for the PDC controller. From Fig. 7, it demonstrates that the PDC/CCC provided the best contour tracking performance out of other three controllers for the diamond contour motion. Similar conclusion was obtained for the zigzag contour.

https://doi.org/10.1017/S0263574714000769 Published online by Cambridge University Press

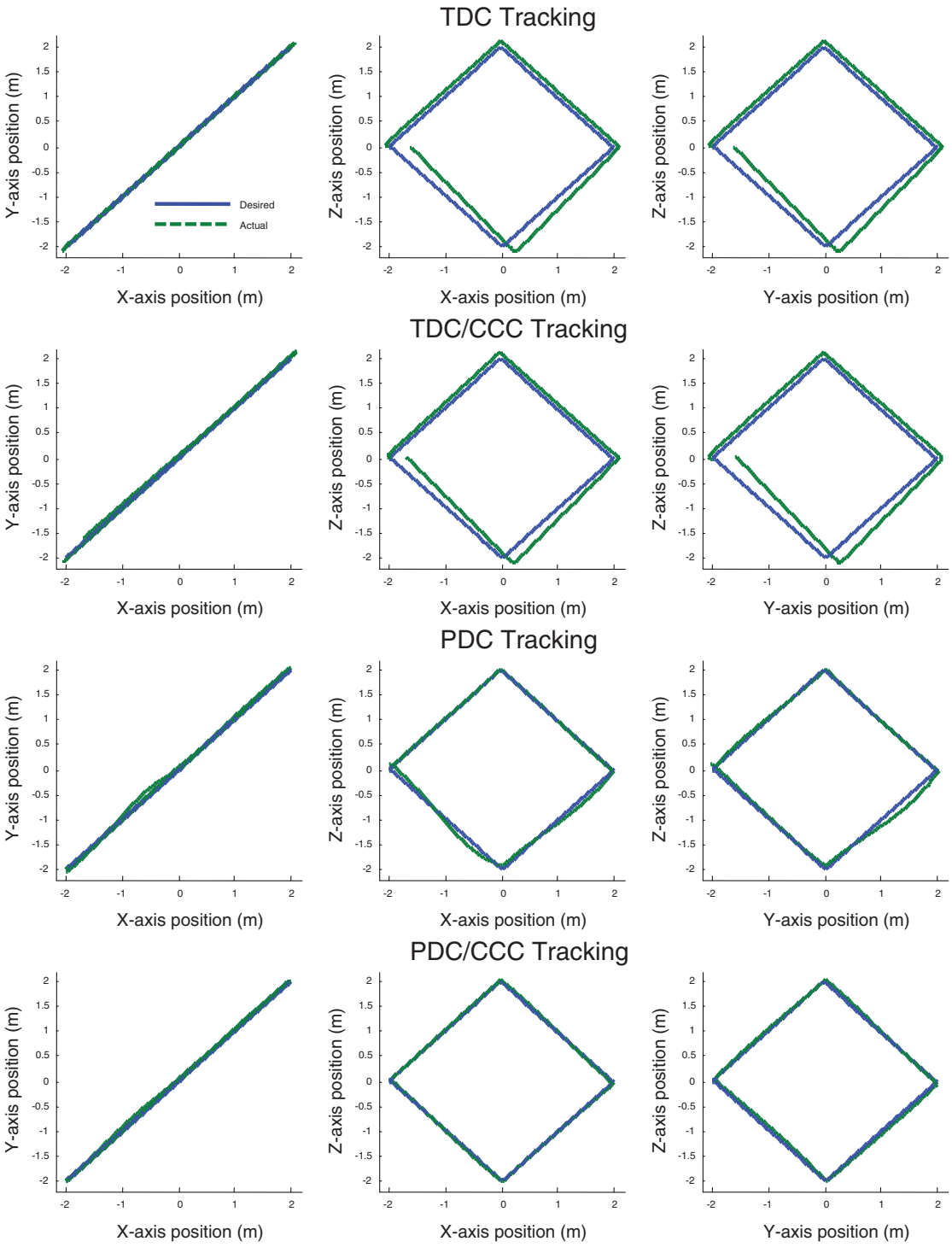


Fig. 7. Contour tracking results with amplified errors for diamond motion.

4.3. Circular motion contour tracking

For a 3D circular contour motion, the radius in each axis is set to 0.5 m and the total time duration T is set to 10 s for a full circle tracking. To verify the effectiveness of the proposed PDC/CCC, two cases with different derivative gains are tested in the simulation first and the control gains are set as follows:

$$K_{Pi}^{t} = K_{Pi}^{p} = K_{Pi}^{c} = 80,000 \quad \text{and} \quad K_{li}^{t} = K_{li}^{p} = 50,000.$$

https://doi.org/10.1017/S0263574714000769 Published online by Cambridge University Press

Table V. Contour tracking performance statistics for circular motion ($\times 10^{-4}$ m).

Controllers	Low derivative gain case				High derivative gain case			
	Overall		Maximum		Overall		Maximum	
	Mean	S.D.	Mean	S.D.	Mean	S.D.	Mean	S.D.
TDC	4.95	2.48	9.57	7.16E-2	4.95	2.56	9.27	6.65E-2
TDC/CCC	5.23	2.50	9.65	4.95E-2	5.40	2.52	9.33	7.70E-2
PDC	1.73	0.52	2.20	2.71E-5	1.18	0.36	1.52	4.00E-3
PDC/ CCC	1.47	0.49	1.95	4.52E-3	1.14	0.38	1.49	4.00E-3

Low derivative gain case: High derivative gain case:

$$K_{Di}^t = K_{Di}^p = K_{Di}^c = 50,000. \quad K_{Di}^t = K_{Di}^p = K_{Di}^c = 70,000$$

The circular contour tracking simulation was conducted 10 times with the TDC and PDC controllers using the listed control gains to obtain the contour tracking performance indexes. Table V shows the index results for two different derivative gain cases and demonstrates the effectiveness of the derivative gain on the improvement of contour performance. For TDC and TDC/CCC, the maximum contour error was approximately 0.9 mm for both cases, with slight reduction (about 3%) of the maximum contour error for the high derivative gain case. For both PDC controllers, the overall contour performance indexes are about 1/3 that of the TDC controllers for the low derivative gain case and about 1/4 that of the TDC controllers for the high derivative case. Also, it can be seen that the maximum contour errors are much smaller (around 20%) than those of the TDC controllers. All these results demonstrate the effectiveness of the PDC controllers. Furthermore, as the increase of the derivative control gain, the overall performance index and the maximum contour error are smaller compared to the low gain case for the PDC controllers. Such a result is expected for the PDC controllers, as a large derivative control gain has large effect and contour performance improvement for the large relative velocities in PDC compared to the low absolute velocities in TDC.

Figure 8 shows one simulation result for the tracking errors of individual axis based on four different controllers for the low derivative control gain case. From this figure, it is shown that very similar tracking performances are obtained in the Y-axis and Z-axis, because of the same contour motion profiles and similar dynamic model for both Y-axis and Z-axis. The tracking errors controlled by the PDC are about 1/3 of those controlled by the TDC for the circular motion tracking.

Figure 9 shows the contour tracking results in separated planar views where the tracking errors have been magnified by a factor of 100. From this figure, the tracking performance improvements can be easily seen from the TDC to the PDC/CCC, and the PDC/CCC is the best in terms of small tracking errors.

From Fig. 9, one can see that the PDC and PDC/CCC are able to track the circular motion accurately throughout the entire contour in comparison to the TDC controllers. This resulted in smaller final contour error values as shown in Fig. 10. The contour tracking performance of the PDC/CCC is slightly improved over the PDC for the circular contour tracking and both position domain controllers have considerable performance improvement over the TDC controllers. The PDC controllers exceeded the TDC controllers with much lower overall contour errors and much smaller maximum contour errors.

To examine the effect of control gains on the contour tracking performance for the circular motion, 10 simulation tests are conducted using doubled control gains for all the control parameters listed for the high derivative gain case. Table VI lists the statistical results of the contour performance indexes. Compared to the results of the high derivative gain case listed in Table V, the overall performance index and the maximum contour errors are about 50% reduction when doubled control gains are applied. It concludes that the contour errors can be reduced through the increase of control gains as proved in Eq. (40).

https://doi.org/10.1017/S0263574714000769 Published online by Cambridge University Press

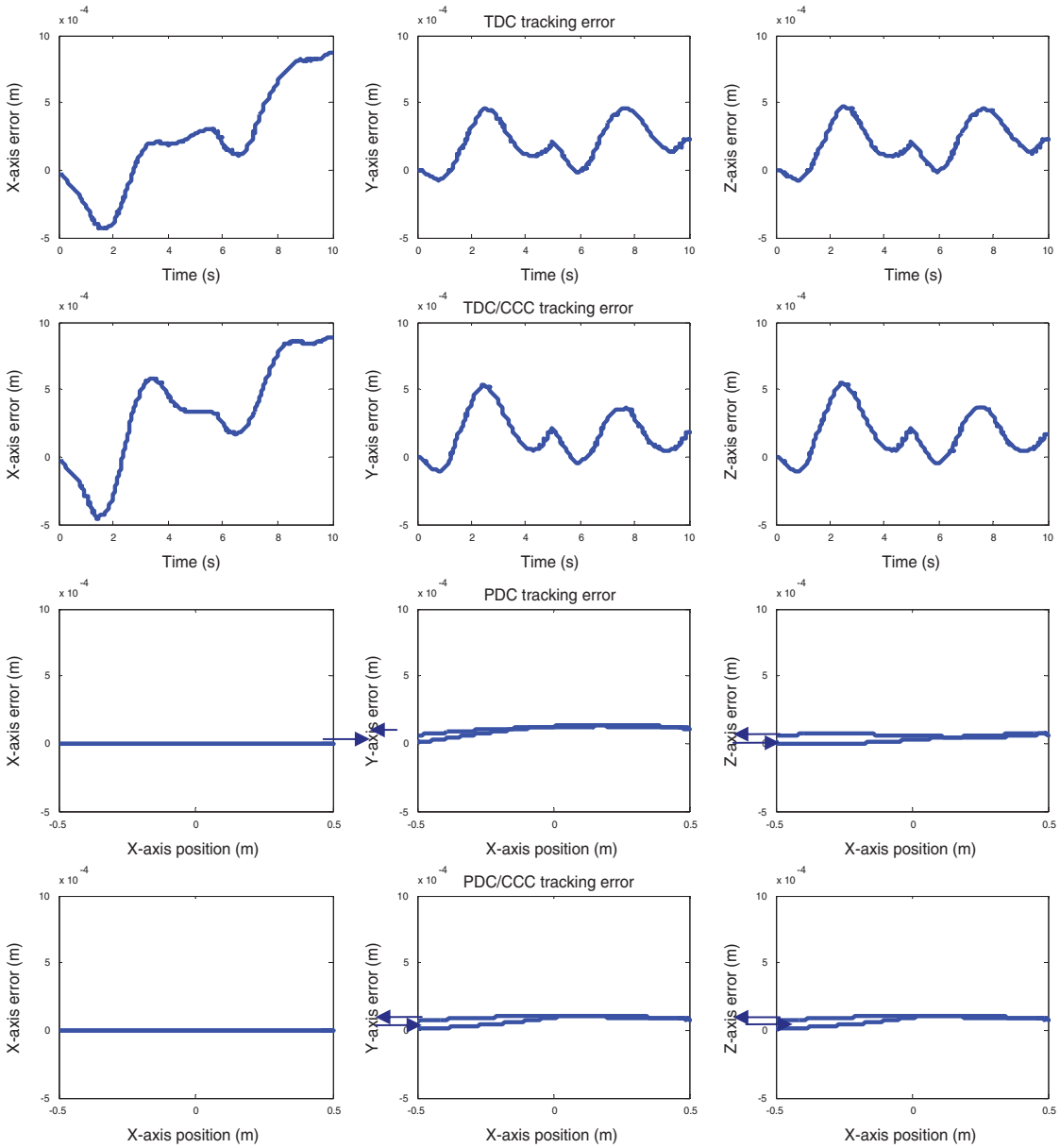


Fig. 8. Axial position tracking of four different controllers for circular contour.

5. Discussions

In the previous section, three different contours are tracked and compared using the different control methods in position domain and time domain. Based on the simulation results, we can see that the proposed PDC/CCC is the best for contour tracking for all three different contours in terms of the maximum contour errors and the mean contour errors, and it demonstrated the effectiveness of the cross-coupled position domain PID control. Compared with the PD-type PDC, the proposed controller provides some flexibility for the choice of control gains, as there are three feedback gains that can be selected.

In the simulation, we assume there is stiffness in each axis that is a general situation for a commercial linear stage. For no spring cases, better contour tracking performances were obtained for all four control methods. Such a result is coincident with the stability analysis, as the stability condition (Eq. (16)) is not related to the stiffness of the spring.

In the proposed PDC/CCC, the cross-coupled part of the developed controller has a PD structure, which is the most common form in the traditional CCC developed in time domain, see refs. [4–7]. It is

https://doi.org/10.1017/S0263574714000769 Published online by Cambridge University Press

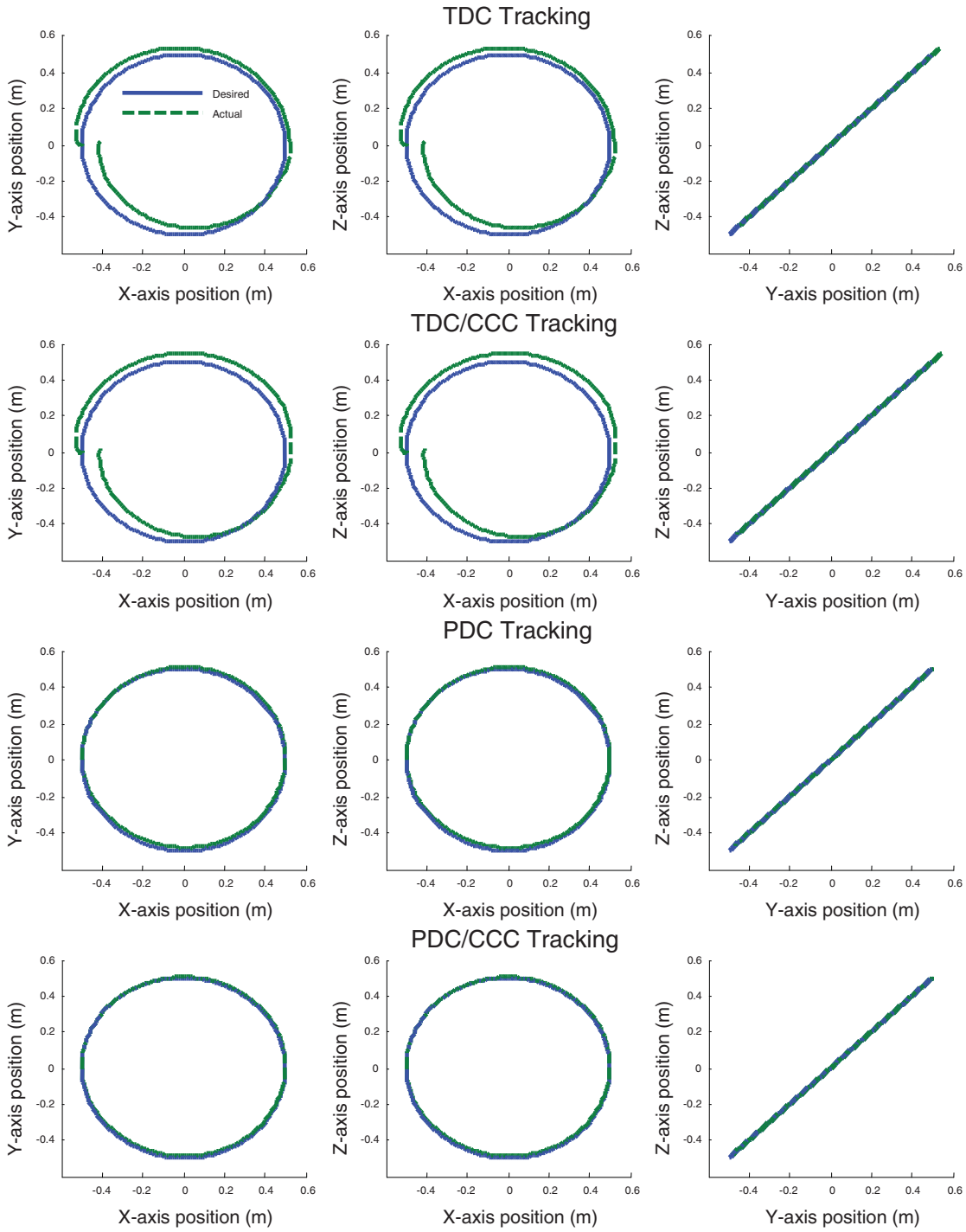


Fig. 9. Contour tracking with amplified errors for circular motion.

possible to include the integral action in the CCC part to form a new PID-type PDC, but the stability analysis needs to be conducted and the selection guide for the integral gain need to be addressed. Solving these issues will be part of future work. Similar to the controllers developed in time domain, for contour tracking control, the most significant control gains are proportional and derivative gains. The integral gain has less contribution for tracking control and cannot be set too high, as constrained in Eq. (16).

It should be mentioned that the proposed PDC is only used for contour tracking, this is one limitation of the PDC. Another limitation is the restriction of the master motion. In the development

https://doi.org/10.1017/S0263574714000769 Published online by Cambridge University Press

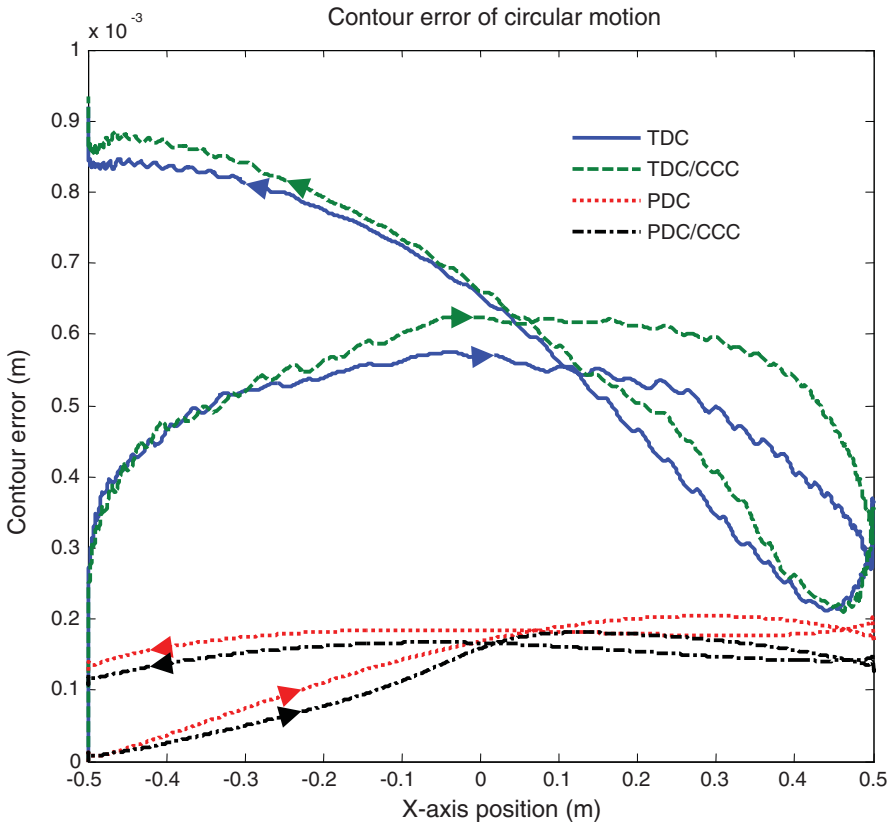


Fig. 10. Contour errors of circular motion.

Table VI. Contour performance statistics for circular motion with doubled control gains ($\times 10^{-4}$ m).

	Overall		Maximum	
Controllers	Mean	S.D.	Mean	S.D.
TDC	2.887	1.584	5.421	0.332
TDC/CCC	3.270	1.561	5.930	0.129
PDC	0.585	0.169	0.768	5.995E-3
PDC/ CCC	0.572	0.189	0.743	4.330E-3

of the PDC, it is assumed that the master motion is in the same direction during the contour tracking process. For more complicated contour tracking problems where the master motion needs to operate in both directions, we can divide the master motion into a few segments to make sure that, for each segment, the master motion is in one direction, as explained in Remark 2.

6. Conclusion

In this paper, a cross-coupled position domain PID controller is proposed and compared to time domain PID/CCC controller for different contour tracking of a 3-DOF CNC machine. In PDC, the motion of a master axis is sampled and used as a reference to develop the position domain dynamic model, thus it yields zero tracking error. Only the tracking errors of the slave motions will contribute to the overall contouring error of the motion. The stability analysis for the proposed cross-coupled position domain PID controller was proved and guidelines for choosing control gains are provided.

From the simulation of two types of motions, a linear motion and a circular motion, it concluded that the cross-coupled PID position domain controller can provide improved contour tracking performances, particularly if the slave axes are controlled through additional CCC. The cross-coupled position domain PID controller was able to provide improved performance in terms of small

https://doi.org/10.1017/S0263574714000769 Published online by Cambridge University Press

tracking error and contouring error over the time domain controllers. The mean contouring error and standard deviation were approximately two times lower than the counterparts in time domain. Results between the position domain controller with and without CCC indicate that smaller tracking error and contouring error were achieved by the PDC/CCC. Further work is needed to demonstrate the effectiveness of the position domain controller on arbitrary contours.

Acknowledgements

This research is supported by the Natural Sciences and Engineering Research Council of Canada (NSERC) through a Discovery Grant to the first author.

References

1. M. W. Spong, S. Hutchinson and M. Vidyasagar, *Robot Modeling and Control* (John Wiley & Sons, New York, 2006).
2. J. J. Craig, *Introduction to Robotics: Mechanics and Control* (Addison-Wesley, Massachusetts, 1986).
3. P. Kelly, "PD control with desired gravity compensation of robotic manipulators: A review," *Int. J. Robot. Res.* **6**(5), 660–672 (1997).
4. Y. Koren, "Cross-coupled biaxial computer control for manufacturing systems," *ASME J. Dyn. Syst. Meas. Control* **102**(4), 265–272 (1980).
5. Y. Koren and Ch. Ch. Lo, "Variable-gain cross-coupling controller for contouring," *CIRP Ann.- Manuf. Technol.* **40**(1), 371–374 (1991).
6. R.W. Fang and J. S. Chen, "Cross-coupling control for a direct-drive robot," *JSMA, Series C* **45**(3), 749–757 (2002).
7. K. L. Barton and A. G. Alleyne, "A cross-coupled iterative learning control design for precision motion control," *IEEE Control Syst. Technol.* **16**(6), 1218–1230 (2008).
8. K. E. Årzén, "A Simple Event-Based PID Controller," *Proceedings of the 14th IFAC World Congress, Beijing, China* (1999) pp. 423–428.
9. K. J. Åström, "Event Based Control," **In**: *Analysis and Design of Nonlinear Control Systems* (A. Astolfi and L. Marconi, eds.) (Springer, 2008) pp. 127–147.
10. M. Nakano, J. H. She, Y. Mastuo and T. Hlno, "Elimination of position-dependent disturbances in constant-speed-rotation control systems," *Control Eng. Pract.* **4**(9), 1241–1248 (1996).
11. W. Heemels, J. Sandee and P. Van Den Bosch, "Analysis of event-driven controllers for linear systems," *Int. J. Control* **81**(4), 571–590 (2008).
12. P. R. Ouyang, W. J. Zhang and F. X. Wu, "Nonlinear PD Control for Trajectory Tracking with Consideration of the Design for Control Methodology," *Proceedings of 2002 IEEE ICRA*, Washington, USA (May 9–11, 2002) pp. 4126–4131.
13. P. R. Ouyang, T. Dam, J. Huang and W.J. Zhang, "Contour tracking control in position domain," *Mechatronics* **22**(7), 934–944 (2012).
14. P. R. Ouyang, V. Pano and T. Dam, "PID position domain control for contour tracking," *Int. J. Syst. Sci.* (2013). http://dx.doi.org/10.1080/00207721.2013.775385.
15. T. Dam and P. R. Ouyang, "Position Domain Contour Tracking with Cross-coupled Control," *2012 IEEE 21st International Symposium on Industrial Electronics, Hangzhou, China* (May 28–31, 2012) pp. 1303–1308.
16. J. J. E. Slotine and W. P. Li, *Applied Nonlinear Control* (Prentice-Hall, Inc., New Jersey, 1991).
17. H. K. Khalil, *Nonlinear Systems*, 3rd ed. (Prentice Hall, New Jersey, 2002).

https://doi.org/10.1017/S0263574714000769 Published online by Cambridge University Press